Optimizing nutrient channel spacing and revisiting TGF-beta in large engineered cartilage constructs

Alexander D. Cigan, PhD, **Robert J. Nims, MS**, **Gordana Vunjak-Novakovic, PhD**, **Clark T. Hung, PhD**, and **Gerard A. Ateshian, PhD**
Departments of Mechanical Engineering, Biomedical Engineering and Medicine, Columbia University, New York, NY 10027

Abstract

Cartilage tissue engineering is a promising approach to treat osteoarthritis. However, current techniques produce tissues too small for clinical relevance. Increasingly close-packed channels have helped overcome nutrient transport limitations in centimeter-sized chondrocyte-agarose constructs, yet optimal channel spacings to recapitulate native cartilage compositional and mechanical properties in constructs this large have not been identified. Transient active TGF-β treatment consistently reproduces native compressive Young's modulus (E_Y) and glycosaminoglycan (GAG) content in constructs, but standard dosages of 10 ng/mL exacerbate matrix heterogeneity. To ultimately produce articular layer-sized constructs, we must first optimize channel spacing and investigate the role of TGF-β in the utility of channels. We cultured $\varnothing$10 mm constructs with 0, 12, 19, or 27 nutrient channels ($\varnothing$1 mm) for 6-8 weeks with 0, 1, or 10 ng/mL TGF-β; subsequently we analyzed them mechanically, biochemically, and histologically. Constructs with 12 or 19 channels grew the most favorably, reaching $E_Y = 344 \pm 113$ kPa and GAG and collagen contents of $10.8\% \pm 1.2\%$ and $2.2\% \pm 0.2\%$ of construct wet weight, respectively. Constructs with 27 channels had significantly less deposited GAG than other groups. Channeled constructs given 1 or 10 ng/mL TGF-β developed similar properties. Without TGF-β, constructs with 0 or 12 channels exhibited properties that were indistinguishable, and lower than TGF-β-supplemented constructs. Taken together, these results emphasize that nutrient channels are effective only in the presence of TGF-β, and indicate that spacings equivalent to 12 channels in $\varnothing$10 mm constructs can be employed in articular-layersized constructs with reduced dosages of TGF-β.

Keywords

Tissue Engineering; Cartilage; Agarose; Chondrocytes; Nutrient Transport; Growth Factors

Corresponding author: Gerard A. Ateshian, PhD, Professor of Mechanical Engineering and Biomedical Engineering, Columbia University, 500 West 120th Street, Room 220, New York, NY 10027 USA, Tel: +1 (212) 854-8602 | Fax: +1 (212) 854-3304, ateshian@columbia.edu.

Conflict of Interest Statement

The authors have no conflicts of interest to disclose.

Introduction

Cartilage tissue engineering is a promising approach to treat osteoarthritis, a debilitating joint disease affecting over 27 million Americans and many more worldwide (Lawrence et al., 2008). Current cartilage tissue engineering (CTE) is a promising technique for recapitulating cartilage tissue *in vitro* (Buschmann et al., 1999; Hu and Athanasiou, 2006; Langer and Vacanti, 1993; Moutos and Guilak, 2009; Mouw et al., 2005; Paige and Vacanti, 1995; Talukdar et al., 2011) which has reproduced native compressive Young's moduli (E_Y) and glycosaminoglycan (GAG) contents in $\sim\varnothing 4$ mm chondrocyte-agarose constructs (Byers et al., 2008). However, osteoarthritis (OA) is often asymptomatic until cartilage lesions reach $\sim\varnothing 25$ mm (Moisio et al., 2009), and therefore the ability to grow constructs of this size is ultimately necessary for clinical relevance of CTE. Previous attempts to culture articular layer-sized constructs exhibited matrix heterogeneity due to poor nutrient availability at construct interiors (Hung et al., 2003; Hung et al., 2004).

The incorporation of nutrient channels reduces transport distances within constructs (Bian et al., 2009; Buckley et al., 2009). We previously demonstrated beneficial effects of placing 3 (CH3) or 12 (CH12) evenly spaced $\varnothing 1$ mm channels in $\varnothing 10$ mm juvenile bovine chondrocyteagarose constructs, compared to channel-free controls (CH0) (Bian et al., 2009; Cigan et al., 2014; Nims et al., 2015). Computational growth models of constructs with increasing numbers of channels up to CH12 (Nims et al., 2015) predicted increased glucose availability, a previously shown marker for construct growth (Cigan et al., 2013; Heywood et al., 2006; Nims et al., 2014), and concomitant increases in matrix synthesis. Later experiments supported these trends, though disparities in tissue growth due to channel spacing were greatly under-predicted by glucose availability alone and had no apparent plateaus (Nims et al., 2015).

For a given hydrogel size and cell seeding density, increasing the number of channels reduces the total cell number, and the benefits of heightened nutrient availability become offset. Thus an optimum channel density exists, which has yet to be determined. Recently, we demonstrated that conventional supplementation of constructs with 10 ng/mL active TGF-β, which permits the achievement of native E_Y and GAG content by constructs in serum-free media (Byers et al., 2008), contributes substantially to matrix heterogeneity within constructs (Albro et al., 2016), placing new emphasis on the utility of channels in CTE systems requiring TGF-β.

Ultimately, we aim to employ channels and TGF-β to cultivate articular layer-sized constructs (~ 10 cm^2) that are clinically relevant for treatment of OA. To achieve this aim, our two immediate objectives are to more fully elucidate the interplay between channels and TGF-β, and to identify optimal channel spacing for this culture system before scaling up further. To these ends, we 1) cultivated CH0 and CH12 constructs without TGF-β and contrasted the results with TGF-β-supplemented constructs, and 2) placed greater numbers of channels (beyond CH12) in $\varnothing 10$ mm constructs to explore the upper limits of channel effectiveness.

Methods

Custom Mold Fabrication

CH0 and CH12 constructs were cast with previously described PTFE/steel/glass molds (Cigan et al., 2014). Closer-set channel configurations were designed such that whole numbers of triangularly-packed $\varnothing 1$ mm channels could be symmetrically contained within $\varnothing 10 \times 2.3$ mm cylindrical constructs. The resulting channels were spaced 1.83 mm or 1.54 mm (center-to-center) to yield 19 or 27 channels (CH19 or CH27), respectively. These molds (Figure 1) were designed in Solidworks (Dassault Systèmes, Waltham, MA), manufactured from polyacrylate material (VeroWhitePlus RGD835) by a 3D printer (Objet24, Stratasys, Eden Prairie, MN), dried overnight under vacuum at 50 °F, and sterilized in 70% ethanol for 10 minutes prior to use.

Culture conditions

Juvenile bovine primary articular chondrocytes were cast with nominal seeding density 60×10^6 cells/mL in 2% w/v agarose as previously described (Cigan et al., 2013). The actual cell seeding densities were measured at 60×10^6 and 45×10^6 cells/mL (Studies 1 and 2, respectively). Experimental groups are depicted in Figure 2. In Study 1, CH0 and CH12 constructs (n = 5 per group) were cast (Cigan et al., 2014) and cultured in ITS media (Cigan et al., 2013) for 42 days without TGF-β. In Study 2, CH0, CH12, CH19, and CH27 constructs (Figure 1C-D) were cast and cultured for 56 days (n = 4 per group) with 10 ng/mL TGF-β3 for the first 14 days; additional CH12 constructs (n = 2) were supplemented instead with 1 ng/mL TGF-β3 (CH12 1ng).

Mechanical, Biochemical, and Histological Analyses

Constructs were tested for E_Y, bisected, and half of each construct was assessed for GAG and collagen contents and cellularity as previously described (Cigan et al., 2014; Farndale et al., 1986; Hollander et al., 1994). GAG and collagen were expressed as either percent of final wet weight (%/ww, a measure of construct composition) or as percent of initial wet weight (%/D0ww, a measure of total matrix deposition). Swelling ratios (SR) were calculated as the ratio of final construct weights to construct day 0 weights. Sagittal sections of remaining half-constructs were taken so as to intersect channels (when possible) and were stained with 0.1% Safranin O (for GAG) or 0.1% Picrosirius Red (for collagen) as previously described (Kelly et al., 2006).

Statistics

Study 1 constructs (CH0 and CH12) were compared by unpaired Student's t-test for E_Y, SR, and %/ww GAG and collagen. In Study 2, groups receiving 10 ng/mL TGF-β were analyzed by one-way ANOVA ($\alpha = 0.05$) with channel configuration as the independent factor, and with E_Y, SR, and GAG and collagen contents (by %/ww and %/D0ww) as dependent variables. Tukey's HSD post hoc tests were instituted upon determination of significance ($p < 0.05$). In a separate analysis, CH12 1ng and CH12 10ng constructs were compared by t-test similarly as above.

Results

Effects of channels without TGF-β

In Study 1, CH0 and CH12 constructs receiving no TGF-β had similar E_Y (100 ± 27 kPa, $p = 0.87$; Figure 3A), GAG (5.0 ± 0.7 %/ww, $p = 0.23$; Figure 3C), and collagen (1.7 ± 0.3 %/ww, $p = 0.42$; Figure 3D). CH12 constructs had higher SR (1.28 ± 0.07) than CH0 (1.17 ± 0.04, $p < 0.05$; Figure 3B).

Effects of channel configuration

Morphology and histology—All Study 2 constructs were opaque and resembled native cartilage (Figure 2). Channels tended to fill in, in some instances entirely, with dark staining for collagen often present at the margins (Figures 2, 4). CH0 constructs cracked at their centers and formed fluid-filled cavities (Figure 4A-B), with cracks reaching the surface (Figure 2). Distributions of GAG and collagen were uniform in channeled constructs (Figure 4E-J). Channels influenced SR ($p < 0.0001$, Figure 5A), with CH27 constructs swelling the least (SR: 1.5 ± 0.4, $p < 0.0005$) and CH0 swelling the most (SR: 3.0 ± 0.1, $p < 0.05$).

Functional properties—Channeled constructs receiving 10 ng/mL TGF-β developed E_Y ~340 kPa (Figure 5B); CH0 moduli were much lower (66 ± 57 kPa), but because two CH0 constructs could not be reliably mechanically tested due to extreme surface irregularities, no statistical effect of channel spacing was shown ($p = 0.10$). All constructs had similar %/ww GAG (10.3 ± 1.2 %/ww, $p = 0.26$; Figure 5C) and collagen (2.2 ± 0.2 %/ww, $p = 0.51$; Figure 5E), and %/D0ww collagen (4.7 ± 0.6 %/D0ww, $p = 0.08$; Figure 5F). %/D0ww GAG was influenced by channel spacing ($p < 0.0005$, Figure 5D), with CH27 having the lowest (15.3 ± 3.9 %/D0ww, $p < 0.005$) and the other constructs being similar (25.8 ± 2.8 %/D0ww, $p > 0.46$).

Reduced TGF-β

CH12 1ng constructs developed similar morphological and histological features as CH12 10ng constructs (Figures 2, 4C-F), though they swelled less (Table 1). Lower TGF-β dosage yielded E_Y over twice as high as constructs receiving standard 10 ng/mL dosages, though this was not statistically significant (Table 1). CH12 1ng had less %/D0ww GAG than CH12 10ng, but similar %/ww GAG, %/ww collagen, and %/D0ww collagen (Table 1).

Discussion

A primary objective of CTE studies is to recapitulate cartilage's native mechanical properties and matrix content. The E_Y and GAG contents of TGF-β-supplemented, channeled constructs in this study (~347-705 kPa and ~10%/ww, respectively) reached or exceeded levels typical of native cartilage (250-730 kPa and 1-5%/ww, respectively), while collagen contents (~2.4%/ww) were below native (~10%/ww) (Canal Guterl et al., 2010; Fetter et al., 2006; Krishnan et al., 2003; Treppo et al., 2000). Together with ∅10 mm constructs of our previous experiments (Cigan et al., 2014; Nims et al., 2015), they possess the highest E_Y and GAG reported to date in constructs of their size. In our previous study using 10 ng/mL TGF-β, CH12 constructs contained over twice as much GAG and collagen

as CH0 constructs (Nims et al., 2015). The present results of Study 1 indicate that when TGF-β is withheld, nutrient channels are ineffective, suggesting that TGF-β is critically responsible for the beneficial effects of nutrient channels when glucose supplementation is plentiful (Nims et al., 2015). However, functional properties of TGF-β-free constructs were low compared to constructs receiving 1 or 10 ng/mL TGF-β (Figures 2-3, 5), as demonstrated previously in constructs cultured over similar durations as the present study (42-56 days) (Byers et al., 2008; Nims et al., 2014), reinforcing the importance of TGF-β and therefore of nutrient channels in chondrocyte-agarose constructs.

To investigate denser channel configurations, molds were 3D-printed for CH19 and CH27 constructs (Figure 1). In contrast to previously-used plastic/metal molds which were labor- and time-intensive to fabricate (Cigan et al., 2014), this represents a precise, rapid, and economical method of producing various channel configurations. CH27 constructs produced substantially less GAG than all other groups (Figure 5D), and though they still contained similar levels of deposited collagen as other constructs, much of their overall growth occurred at the construct peripheries, outside the channel grid, suggesting that an upper limit for packing of channels had been reached, since the beneficial effects of shorter nutrient transport distances were outweighed by the lower initial cell population. Though CH12 and CH19 constructs developed similar properties, CH19 constructs were more fragile to handle and therefore we will employ the spacing used for CH12 constructs in our future experiments growing articular layersized constructs.

Constructs without channels performed poorly, albeit for different reasons than observed previously (Bian et al., 2009; Cigan et al., 2014; Nims et al., 2015). Compared to our prior experiment in which CH0 constructs produced less matrix and swelled to lesser extents (Nims et al., 2015), the current CH0 constructs swelled extensively at their peripheries, leaving large, fluid-filled cracks at their centers. However, we believe the inadequacies of CH0 constructs from both studies stem from poor nutrient availability at construct interiors, lending credence to channels as a strategy to enhance tissue growth.

CH12 constructs cultured with lower dosages of TGF-β (1 ng/mL) had similar GAG and collagen contents to those with standard dosages of 10 ng/mL (Table 1). Even though the lower dose resulted in less overall GAG synthesis (%/D0ww), the similarly reduced swelling may have been responsible for higher E_Y due to a more uniformly cylindrical shape, making more complete contact with testing platens. Furthermore, we recently demonstrated that quelling construct swelling can reduce damage to deposited collagen fibrils and increase E_Y (Nims et al., 2016). We deem the properties attained by CH12 1ng constructs acceptable, particularly in light of our recent findings that 10 ng/mL TGF-β exacerbates matrix heterogeneity (Albro et al., 2016), and considering that reducing TGF-β requirements tenfold greatly reduces the cost of cultivating large CTE constructs in sufficient media volumes (Nims et al., 2015), and will facilitate the culture of even larger-scale constructs.

The cells used in this study were of juvenile bovine origin. Though CTE methods with human cells are ultimately necessary to treat OA, juvenile bovine chondrocytes represent a highly useful and well-established model system (Freed and Vunjak-Novakovic, 1997; Mauck et al., 2000). Further, juvenile chondrocytes have shown promise for clinical

applications in allogeneic transplantation (Adkisson et al., 2010). Ongoing and future studies by our group seek to translate results in bovine model systems to human chondrocytes (Cigan et al., 2016; O'Connell et al., 2015).

Ultimately, we aim to employ nutrient channels to produce high-quality, human articular layer-sized CTE constructs with mechanical and biochemical properties reflective of native cartilage. The results of the current study expanded on prior results to provide valuable insights for cultivating channeled CTE constructs. An optimum channel spacing for enhancing construct growth was experimentally determined and a strong relationship was demonstrated between TGF-β supplementation and channel effectiveness. Finally, a tenfold reduction of conventional TGF-β dosages yielded constructs of similar quality for a fraction of the cost. Together with our previous work, these findings will help enable the cultivation of CTE tissues sufficiently large to repair entire joints damaged by OA.

Acknowledgments

References

Adkisson HD, Martin JA, Amendola RL, Milliman C, Mauch KA, Katwal AB, Seyedin M, Amendola A, Streeter PR, Buckwalter JA. The potential of human allogeneic juvenile chondrocytes for restoration of articular cartilage. Am J Sports Med. 2010; 38:1324–1333. [PubMed: 20423988]

Albro MB, Nims RJ, Durney KM, Cigan AD, Shim JJ, Vunjak-Novakovic G, Hung CT, Ateshian GA. Heterogeneous engineered cartilage growth results from gradients of media-supplemented active TGF-beta and is ameliorated by the alternative supplementation of latent TGF-beta. Biomaterials. 2016; 77:173–185. [PubMed: 26599624]

Bian L, Angione SL, Ng KW, Lima EG, Williams DY, Mao DQ, Ateshian GA, Hung CT. Influence of decreasing nutrient path length on the development of engineered cartilage. Osteoarthritis and Cartilage. 2009; 17:677–685. [PubMed: 19022685]

Buckley CT, Thorpe SD, Kelly DJ. Engineering of large cartilaginous tissues through the use of microchanneled hydrogels and rotational culture. Tissue Engineering Part A. 2009; 15:3213–3220. [PubMed: 19374490]

Buschmann MD, Kim Y-J, Wong M, Frank E, Hunziker EB, Grodzinsky AJ. Stimulation of Aggrecan Synthesis in Cartilage Explants by Cyclic Loading Is Localized to Regions of High Interstitial Fluid Flow. Archives of biochemistry and biophysics. 1999; 366:1–7. [PubMed: 10334856]

Byers BA, Mauck RL, Chiang IE, Tuan RS. Transient exposure to transforming growth factor beta 3 under serum-free conditions enhances the biomechanical and biochemical maturation of tissue-engineered cartilage. Tissue Engineering Part A. 2008; 11:1821–1834. [PubMed: 18611145]

Canal Guterl C, Hung CT, Ateshian GA. Electrostatic and non-electrostatic contributions of proteoglycans to the compressive equilibrium modulus of bovine articular cartilage. Journal of Biomechanics. 2010; 43:1343–1350. [PubMed: 20189179]

Cigan AD, Nims RJ, Albro MB, Esau JD, Dreyer MP, Vunjak-Novakovic G, Hung CT, Ateshian GA. Insulin, ascorbate, and glucose have a much greater influence than transferrin and selenous acid on the in vitro growth of engineered cartilage in chondrogenic media. Tissue Engineering Part A. 2013; 19:1941–1948. [PubMed: 23544890]

Cigan AD, Nims RJ, Albro MB, Vunjak-Novakovic G, Hung CT, Ateshian GA. Nutrient channels and stirring enhanced the composition and stiffness of large cartilage constructs. Journal of Biomechanics. 2014; 47:3847–3854. [PubMed: 25458579]

Cigan AD, Roach BL, Nims RJ, Tan AR, Albro MB, Stoker AM, Cook JL, Vunjak-Novakovic G, Hung CT, Ateshian GA. High seeding density of human chondrocytes in agarose produces tissue-engineered cartilage approaching native mechanical and biochemical properties. Journal of Biomechanics. 2016 (In Press), doi: http://dx.doi.org/10.1016/j.jbiomech.2016.1004.1039.

Farndale RW, Buttle DJ, Barrett AJ. Improved quantitation and discrimination of sulphated glycosaminoglycans by use of dimethylmethylene blue. Biochimica et Biophysica Acta. 1986; 883:173–177. [PubMed: 3091074]

Fetter NL, Leddy HA, Guilak F, Nunley JA. Composition and transport properties of human ankle and knee cartilage. Journal of orthopaedic research : official publication of the Orthopaedic Research Society. 2006; 24:211–219. [PubMed: 16435350]

Freed LE, Vunjak-Novakovic G. Microgravity tissue engineering. In Vitro Cellular & Developmental Biology-Animal. 1997; 33:381–385. [PubMed: 9196897]

Heywood HK, Bader DL, Lee DA. Glucose concentration and medium volume influence cell viability and glycosaminoglycan synthesis in chondrocyte-seeded alginate constructs. Tissue Engineering. 2006; 12:3487–3496. [PubMed: 17518685]

Hollander AP, Heathfield TF, Webber C, Iwata Y, Bourne R, Rorabeck C, Poole AR. Increased damage to type II collagen in osteoarthritic articular cartilage detected by a new immunoassay. Journal of Clinical Investigation. 1994; 93:1722–1732. [PubMed: 7512992]

Hu JC, Athanasiou KA. A self-assembling process in articular cartilage tissue engineering. Tissue Engineering. 2006; 12:969–979. [PubMed: 16674308]

Hung CT, Lima EG, Mauck RL, Takai E, LeRoux MA, Lu HH, Stark RG, Guo XE, Ateshian GA. Anatomically shaped osteochondral constructs for articular cartilage repair. Journal of Biomechanics. 2003; 36:1853–1864. [PubMed: 14614939]

Hung CT, Mauck RL, Wang CC, Lima EG, Ateshian GA. A paradigm for functional tissue engineering of articular cartilage via applied physiologic deformational loading. Annals of Biomedical Engineering. 2004; 32:35–49. [PubMed: 14964720]

Kelly TA, Ng KW, Wang CC, Ateshian GA, Hung CT. Spatial and temporal development of chondrocyte-seeded agarose constructs in free-swelling and dynamically loaded cultures. Journal of Biomechanics. 2006; 39:1489–1497. [PubMed: 15990101]

Krishnan R, Park S, Eckstein F, Ateshian GA. Inhomogeneous cartilage properties enhance superficial interstitial fluid support and frictional properties, but do not provide a homogeneous state of stress. Journal of biomechanical engineering. 2003; 125:569–577. [PubMed: 14618915]

Langer R, Vacanti JP. Tissue engineering. Science. 1993; 260:920–926. [PubMed: 8493529]

Lawrence RC, Felson DT, Helmick CG, Arnold LM, Choi H, Deyo RA, Gabriel S, Hirsch R, Hochberg MC, Hunder GG, Jordan JM, Katz JN, Kremers HM, Wolfe F. Estimates of the prevalence of arthritis and other rheumatic conditions in the United States. Part II. Arthritis and Rheumatism. 2008; 58:26–35. [PubMed: 18163497]

Mauck RL, Soltz MA, Wang CC, Wong DD, Chao PH, Valhmu WB, Hung CT, Ateshian GA. Functional tissue engineering of articular cartilage through dynamic loading of chondrocyte-seeded agarose gels. Journal of biomechanical engineering. 2000; 122:252–260. [PubMed: 10923293]

Moisio K, Eckstein F, Chmiel JS, Guermazi A, Prasad P, Almagor O, Song J, Dunlop D, Hudelmaier M, Kothari A, Sharma L. Denuded subchondral bone and knee pain in persons with knee osteoarthritis. Arthritis and Rheumatism. 2009; 50:3703–3710. [PubMed: 19950284]

Moutos FT, Guilak F. Functional properties of cell-seeded three-dimensionally woven poly (ε-caprolactone) scaffolds for cartilage tissue engineering. Tissue Engineering Part A. 2009; 16:1291–1301. [PubMed: 19903085]

Mouw JK, Case ND, Guldberg RE, Plaas AH, Levenston ME. Variations in matrix composition and GAG fine structure among scaffolds for cartilage tissue engineering. Osteoarthritis and Cartilage. 2005; 13:828–836. [PubMed: 16006153]

Nims RJ, Cigan AD, Albro MB, Hung CT, Ateshian GA. Synthesis rates and binding kinetics of matrix products in engineered cartilage constructs using chondrocyte-seeded agarose gels. Journal of Biomechanics. 2014; 47:2165–2172. [PubMed: 24284199]

Nims RJ, Cigan AD, Albro MB, Vunjak-Novakovic G, Hung CT, Ateshian GA. Matrix Production in Large Engineered Cartilage Constructs Is Enhanced by Nutrient Channels and Excess Media Supply. Tissue Engineering Part C. 2015; 21:747–757.

Nims RJ, Durney KM, Cigan AD, Dusséaux A, Hung CT, Ateshian GA. Continuum theory of fibrous tissue damage mechanics using bond kinetics: application to cartilage tissue engineering. Interface Focus. 2016; 6doi: 10.1098/rsfs.2015.0063

O'Connell GD, Tan AR, Cui V, Bulinski JC, Cook JL, Attur M, Abramson SB, Ateshian GA, Hung CT. Human chondrocyte migration behaviour to guide the development of engineered cartilage. J Tissue Eng Regen Med. 2015; doi: 10.1002/term.1988

Paige KT, Vacanti CA. Engineering new tissue: formation of neo-cartilage. Tissue Engineering. 1995; 1:97–106. [PubMed: 19877919]

Talukdar S, Nguyen QT, Chen AC, Sah RL, Kundu SC. Effect of initial cell seeding density on 3D-engineered silk fibroin scaffolds for articular cartilage tissue engineering. Biomaterials. 2011; 32:8927–8937. [PubMed: 21906805]

Treppo S, Koepp H, Quan EC, Cole AA, Kuettner KE, Grodzinsky AJ. Comparison of biomechanical and biochemical properties of cartilage from human knee and ankle pairs. Journal of Orthopaedic Research. 2000; 18:739–748. [PubMed: 11117295]
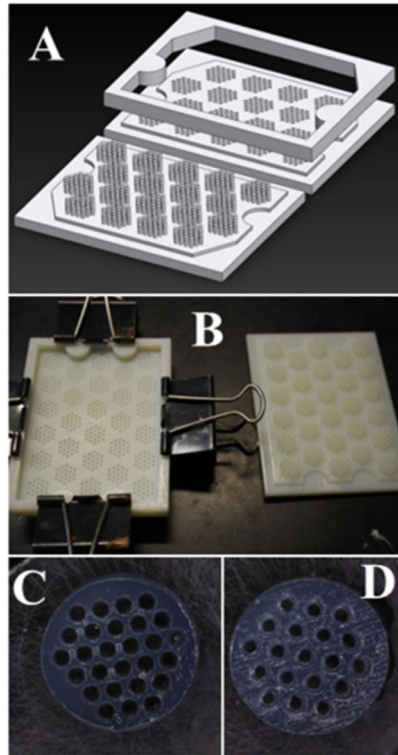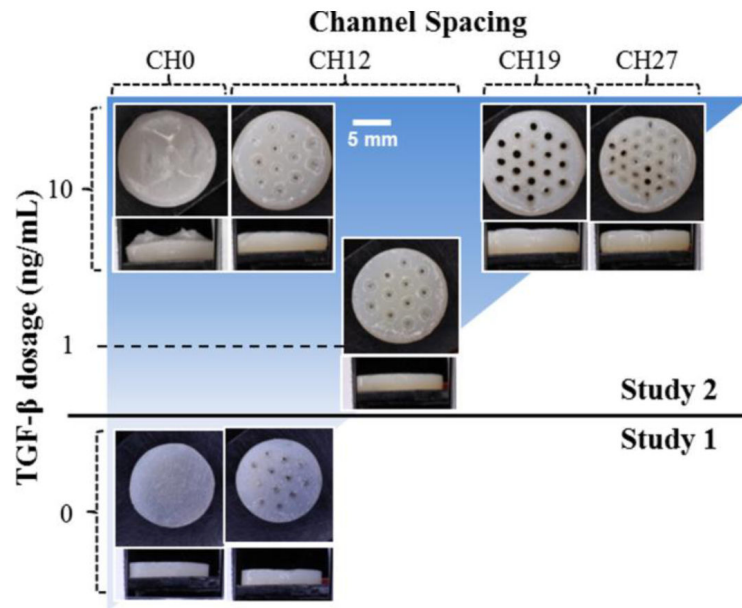
Figure 2.
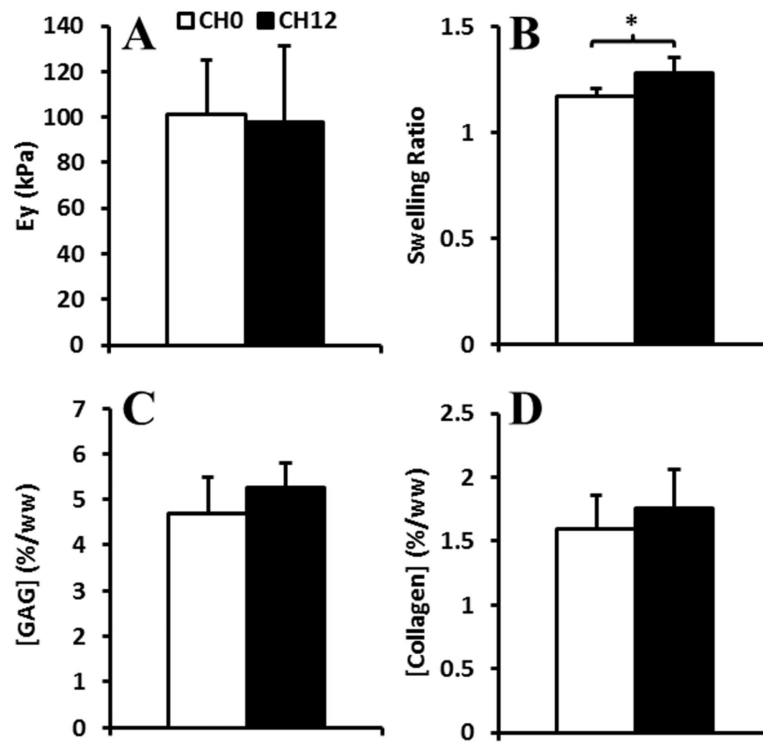Experimental groups and their gross morphologies at day 42 or 56.

Figure 3.
A) E_Y, B) Swelling ratios, and C) GAG and D) collagen contents of Study 1 constructs with 0 or 12 channels cultured without TGF-β.
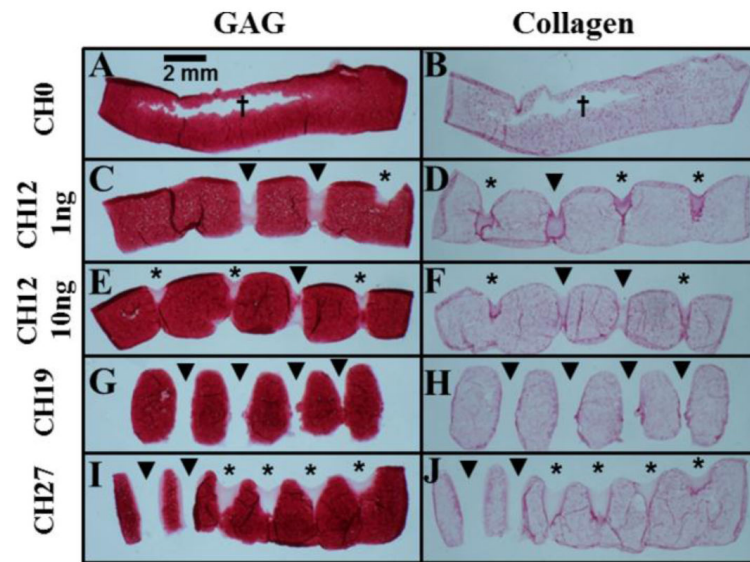
Figure 4.
Histological images of Study 2 constructs, stained for GAG by Safranin O (left) or for collagen by Picrosirius Red (right). Sections through open channels had multiple fragments whose relative spacings may have been distorted by sectioning; Figure 2 provides a more accurate depiction of overall construct morphology. * filled channels, ▼ open channels, † cracks formed in constructs.
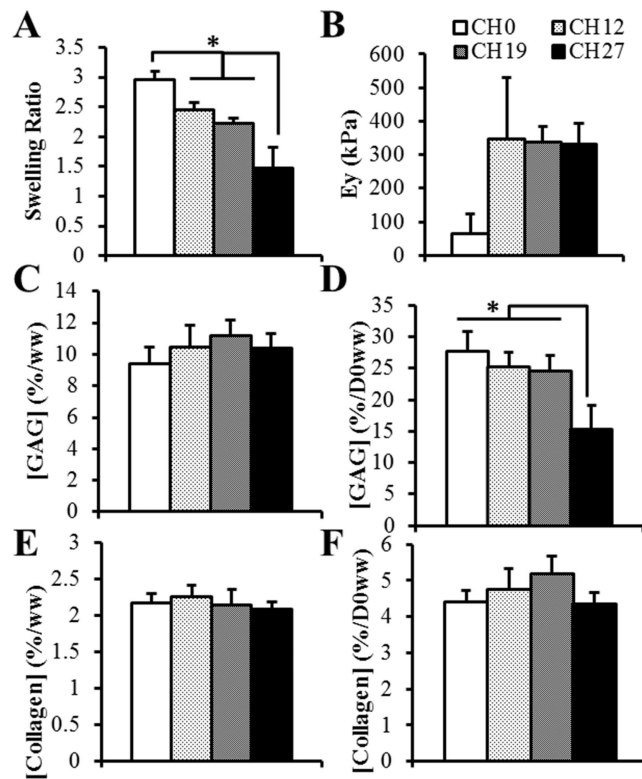
Figure 5.
A) Swelling ratio, B) E_Y, C) %/ww GAG, D) %/D0ww GAG, E) %/ww collagen, and F) %/D0ww collagen for Study 2 constructs. † $p < 0.05$ between CH12 1ng and CH12 10ng, * $p < 0.05$ between different channel configurations.

Table 1

Properties of Study 2 CH12 constructs supplemented with 1 or 10 ng/mL TGF-β.

TGF-β (ng/mL)	Swelling ratio	E_Y (kPa)	GAG (%/ww)	GAG (%/D0ww)	Collagen (%/ww)	Collagen (%/D0ww)
1	2.1 ± 0.1	705 ± 257	9.8 ± 0.8	20.1 ± 0.8	2.4 ± 0.2	4.9 ± 0.8
10	2.4 ± 0.1	347 ± 184	10.4 ± 1.4	25.2 ± 2.2	2.3 ± 0.2	4.7 ± 0.6
p	**0.03**	0.11	0.59	**0.04**	0.33	0.95